P10.5 TAXONOMY AND ANALYSIS OF SIMULATED TORNADO SURFACE MARKS

Michael I. Zimmerman* and David C. Lewellen
West Virginia University, Morgantown, WV

1. INTRODUCTION

The tornado vortex is highly sensitive to properties of the near-surface flow; however, this region is difficult to measure in the field, as Doppler radar cannot probe below about 20 m height. In addition, interpreting Doppler data can be complicated by transient effects and uncertainties about flow asymmetry, debris mass loadings, and differences between scatterer and air velocities near the surface. Properties of near-surface tornado winds are captured to varying degrees by *in-situ* probe measurements, examination of damage to human-made structures, and analysis of forest damage patterns (e.g., Beck and Dotzek (2010)). Here, we extend the previous results of Lewellen and Zimmerman (2008) to show that accumulated patterns of debris deposition and removal, or tornado surface marks (e.g., figs. 1, 2), provide a complementary means of inferring near-surface tornado structure.

A few studies decades ago attempted to infer near-surface tornado structure from surface marks but were limited by uncertainties in their origins (e.g., Agee et al. (1975, 1977); Davies-Jones et al. (1978); Forbes and Wakimoto (1982); Fujita (1966, 1967); Fujita et al. (1967, 1970, 1976); van Tassel (1955)). The most prominent marks were generally assumed to coincide with the paths of individual vortices gathering debris (e.g., fig. 3); however, this historical interpretation of surface marks was cast into doubt through recent large eddy simulations (LES) of debris-laden tornadoes (e.g. Lewellen and Zimmerman (2008)). The shapes of simulated surface marks do not generally coincide with the paths of any particular vortices (either the main vortex or its secondaries, when present). Rather, the sharpest marks were found to result from a convolution in space and time of debris deposition and removal by a handful of near-surface physical processes.

In this work, a much larger LES set (>150 runs) was used to infer the detailed physical origins of the most prominent marks. The simulation set and general simulation technique are summarized in Section 2, and the origins of the marks are outlined in Section 3. All of the types of marks in the historical taxonomy have been encountered. Common classes of marks are reinterpreted in Section 3 in terms of dimensionless parameters governing the tornado corner flow and its debris cloud, allowing generalization to tornado vortices across a wide range of structures, intensities, translation speeds, and debris types. Quantifying properties of surface tracks to deduce flow structure requires distilling the complex information contained; efforts to do so are discussed briefly in Section 4. It is argued in Section 5 that the prospects for inferring near-surface tornado wind fields from the properties of surface marks are most promising when concurrent Doppler measurements are available.

*Corresponding author address: Michael I. Zimmerman, West Virginia University, Department of Physics, Morgantown, WV 26505; e-mail: mzimmer3@mix.wvu.edu.

2. LES MODEL AND SIMULATION SET

The LES model was previously developed as part of a longstanding effort to investigate tornado structure and dynamics; the model and general simulation technique are detailed in Lewellen et al. (2008) (and references therein) and Zimmerman (2010). Typically, steady flow conditions were imposed at the boundaries of a 2 km^3 box. In most simulations, a single mono-disperse debris species was made available at the surface, allowing the debris cloud and air flow to evolve self-consistently to a quasi-steady state. Surface marks were gathered by recording where debris was removed from and deposited to the surface. Other fields were gathered at the surface for comparison, including directional wind measurements, peak and time-integrated measures, and time histories of various flow fields.

Quantities varied included tornado type, size, strength, and translation velocity, gravity, and debris type and availability. Tornado translation speeds typically ranged from 5 m s^{-1} to 25 m s^{-1}, requiring simulation times of hundreds of seconds to generate quasisteady surface tracks of several kilometers length. Typically sand-like debris species were simulated with density ratio to air of $\sigma/\rho \sim 2000$. The primary set of simulations employed stretched grids with finest vertical spacing of 1 m at the surface and finest horizontal spacing of 5 m in the central corner flow. Sensitivity of surface tracks to changes in grid resolution, debris pickup parameterization, and multiple debris species were found to be of at most secondary importance. Also, surface tracks were found to be insensitive to changes in debris type that preserved the debris terminal velocity, w_t, allowing simulation results for small, heavy debris (low d, high σ/ρ) to be reinterpreted in terms of large, light debris such as dried corn stubble (high d, low σ/ρ).

To lowest order four dimensionless parameters most strongly govern the physics producing surface tracks (e.g. Lewellen et al. (2008, 2000); Zimmerman (2010)):

$$S_c \equiv R_c \Gamma_\infty^2 / \Upsilon$$

$$A_v \equiv V_c / w_t$$

$$A_a \equiv V_c^2 / (g R_c)$$

$$A_t \equiv U_{trans} / V_c$$

where V_c and R_c are core swirl velocity and radial scales aloft, Γ_∞ is the far-field angular momentum aloft, Υ is the depleted angular momentum flux through the surface-corner-core flow, g is gravitational acceleration, and U_{trans} is the vortex translation velocity.

S_c is the corner flow swirl ratio and roughly categorizes tornado type. A_v parameterizes the amount of debris slip relative to the air flow; increasing A_v lessens the maximum potential amount of slip. A_a measures the importance of a characteristic radial acceleration relative to gravity. A_t measures the relative importance of the vortex translation speed. The ranges of parameters explored were $0 < S_c < 13$, $1.5 < A_v < 30$, $0.5 < A_a < 77$, $0.05 < A_t < 0.6$.

3. TAXONOMY AND ORIGINS OF MARKS

Surface marks are dominated by deposition under the central vortex, by turbulent inflow rolls, and by fully lofted debris in the far-field, and complicated by subsequent removal and deposition. Deposition signatures were not found to coincide directly with any simple flow measures at the surface such as peak or integrated pressure, turbulence intensity, horizontal or vertical velocity encountered, or secondary vortex paths (e.g., fig. 4). The origins of the most pronounced classes of marks, with relative weights varying with S_c, A_v, A_t, and A_a (c.f. figs. 5,6), are as follows.

Cycloids are created when debris cannot follow the rapid upturn in the corner flow and is dropped in a loose annulus under the central vortex (e.g., figs. 7a,c). To create strong cycloids, debris must be able to reach the corner flow upturn, favored by low A_a (compare e.g., fig. 5h with fig. 6b), and debris must be able to separate from the flow in the corner (otherwise it is lofted), favored by low A_v (e.g., compare figs. 5a,d). The width of cycloidal marks relative to the core diameter aloft increases with S_c (e.g. top row of fig. 6), and spacing and asymmetry increase with A_t (e.g. progressions along columns of fig. 6). Creation of the sharpest cycloidal marks is associated with transient flow convergence along the curved local streamlines.

Trailing arcs (aka “drift marks”) are the signatures (e.g., 7c,e) of surface rolls trailing the main vortex (e.g., figs. 7d,f). Their weight (e.g., relative to cycloids) increases with increasing A_a and A_t. The surface rolls responsible arise in simulations without debris; however, the addition of debris can increase the coherence and lifetime of the rolls, producing trains of alternating removal and deposition. In some cases trailing arcs cover a larger spatial extent or are laid down more intermittently. As with cycloidal marks, generation of the strongest trailing arcs is generally correlated with flow convergence along the local streamlines.

Diffuse far-field swaths occur when fully-lofted debris is redeposited away from the central vortex (e.g. fig. 7g). Vortex tilt produces asymmetry, typically favoring the tornado’s right, increasing with A_t. The amount of lofted debris increases with A_v, causing the weight of far-field swaths (relative to cycloids or trailing arcs) to increase (e.g., the progression across the top row of fig. 5).

Lineation and Scalloping occur when the (translation-relative) righthand part of the deposition annulus is flanked by net removal, leaving a line- or dash-like pattern (e.g. marks aligned along the translation direction in figs. 7c,e). The importance of lineation (e.g. relative to cycloids and trailing arcs) increases with A_t and decreases with A_v and S_c. Very limited debris availability generally produces only a subset of marks favoring scalloping or far-field deposition (fig. 8).

Overall the deposition intensity in surface tracks scales roughly with S_c/A_t and the shift of the vortex center on the ground relative to its position aloft scales with A_t/S_c.

4. QUANTIFYING SURFACE MARKS

Quantifying properties of surface tracks to infer near-surface flow structure requires unraveling their convoluted deposition signatures. Counts of mark spacings along the track, and cross-track profiles averaged along the track have been analyzed to extract information independent of mark shape or phasing. For instance, the cross-track profile of net deposition can be used to infer a near-surface vortex radius when cycloids are present (e.g., fig. 9).

Determining mark shape information independent of multiplicity or phase is more challenging. We have used image-processing techniques to map tracks from the original “along-track vs. cross-track” (x, y) representation to a “mark-angle vs. cross-track” (θ, y) representation and then back to (x, y), giving a mean “fingerprint" of the shapes of the most prominent marks (e.g. fig.

10). The (θ, y) plot can be used directly to determine some quantities; e.g., the relative y position of the crossing point of the two branches is found to correlate with the ratio of U_{trans} and a near-surface swirl velocity. Geometric properties of reconstructed marks may provide additional information about the near-surface flow. Sharp background features such as roads and plough-lines produce distinct signatures in the (θ, y) plot that can sometimes then be filtered out computationally.

5. CONCLUDING REMARKS

In general, the ability to deduce quantitative near-surface flow properties from surface marks would be greatly facilitated by concurrent Doppler radar measurements (providing estimates of V_c, R_c, U_{trans} and vortex center location aloft). Together with the track, these quantities yield direct estimates of A_a and A_t. A_v is less certain due to natural variability in surface debris availability conditions; a video record of debris cloud structure could aid in estimating A_v. An analysis of the track can perhaps be most informative when the underlying surface is relatively uniform but the track appearance evolves significantly, allowing some of the uncertainty in debris properties to drop out of the problem. The presence of cycloidal marks allows the near-surface vortex shift δ_s and radius R_s to be inferred; the time-progressions of δ_s/R_c, R_s/R_c, and A_t, and changes in the qualitative collections of marks observed could then provide quantitative evidence of the evolution of S_c along the tornado's path.

We believe that the prospects are promising enough to warrant renewed documentation of surface marks in the field, particularly when concurrent Doppler measurements are available. The characteristic radius of deposition is often visible in aerial imagery of surface tracks available in the literature (e.g., figs. 1a,b); however, the historical collection of tracks is generally too low in contrast and resolution to enable the more complex quantitative analyses of surface mark shapes. These algorithms are expected to perform more favorably given high-resolution aerial imagery (perhaps >1 pixel per m) taken at a relatively low angle to maximize contrast between modest levels of deposition and removal. Photography from an unmanned aerial vehicle might provide a relatively simple and cost-effective option.

6. ACKNOWLEDGMENTS

This material is based upon work supported by the National Science Foundation under Grants No. ATM-0635681 and AGS-1013154. Any opinions, findings, and conclusions or recommendations expressed in this material are those of the authors and do not necessarily reflect the views of the National Science Foundation.

References

Agee, E. M., J. T. Snow, and P. R. Clare, 1975: Multiple vortex features in the tornado cyclone and the occurrence of tornado families. *Monthly Weather Review*, 552.

Agee, E. M., J. T. Snow, F. S. Nickerson, P. R. Clare, C. R. Church, and L. A. Schaal, 1977: An observational study of the West Lafayette, Indiana, tornado of 20 March 1976. *Monthly Weather Review*, 893.

Beck, V. and N. Dotzek, 2010: Reconstruction of near-surface tornado wind fields from forest damage. *J. Appl. Meteor. Climatol.*, 1517.

Davies-Jones, R. P., D. W. Burgess, L. R. Lemon, and D. Purcell, 1978: Interpretation of surface marks and debris patterns from the 24 May 1973 Union City, Oklahoma tornado. *Monthly Weather Review*, 12.

Forbes, G. S. and R. M. Wakimoto, 1982: A concentrated outbreak of tornadoes, downbursts and microbursts, and implications regarding vortex classification. *Monthly Weather Review*, 220.

Fujita, T. T., 1966: Aerial survey of the Palm Sunday tornadoes of April 11, 1965. *Technical Report SMRP Res. Pap. 49, The University of Chicago*.

— 1967: Estimated wind speeds of the Palm Sunday tornadoes. *Technical Report SMRP Res. Pap. 53, The University of Chicago*.

— 1981: Tornadoes and downbursts in the context of generalized planetary scales. *Journal of the Atmospheric Sciences*, 1511.

Fujita, T. T., D. L. Bradbury, and P. G. Black, 1967: Estimation of tornado wind speed from characteristic ground marks. *Technical Report SMRP Res. Pap. 69, The University of Chicago*.

Fujita, T. T., D. L. Bradbury, and C. F. Thullenar, 1970: Palm Sunday tornadoes of april 11, 1965. *Monthly Weather Review*, 29.

Fujita, T. T., G. S. Forbes, and T. A. Umenhofer, 1976: Close-up view of 20 March 1976 tornadoes: Sinking cloud tops to suction vortices. *Weatherwise*, 116.

Lewellen, D. C., B. Gong, and W. S. Lewellen, 2008: Effects of finescale debris on near-surface tornado dynamics. *Journal of the Atmospheric Sciences*, **65**, 3247.

Lewellen, D. C., W. S. Lewellen, and J. Xia, 2000: The influence of a local swirl ratio on tornado intensification near the surface. *Journal of the Atmospheric Sciences*, **57**, 527.

Lewellen, D. C. and M. I. Zimmerman, 2008: Using simulated tornado surface marks to help decipher near-ground wind fields. *Proceedings of the 24th AMS Conference on Severe Local Storms*, 13.5.

van Tassel, E. L., 1955: The North Platte Valley tornado outbreak of June 27, 1955. *Monthly Weather Review*, 255.

Zimmerman, M., 2010: Doctoral thesis. *West Virginia University*.

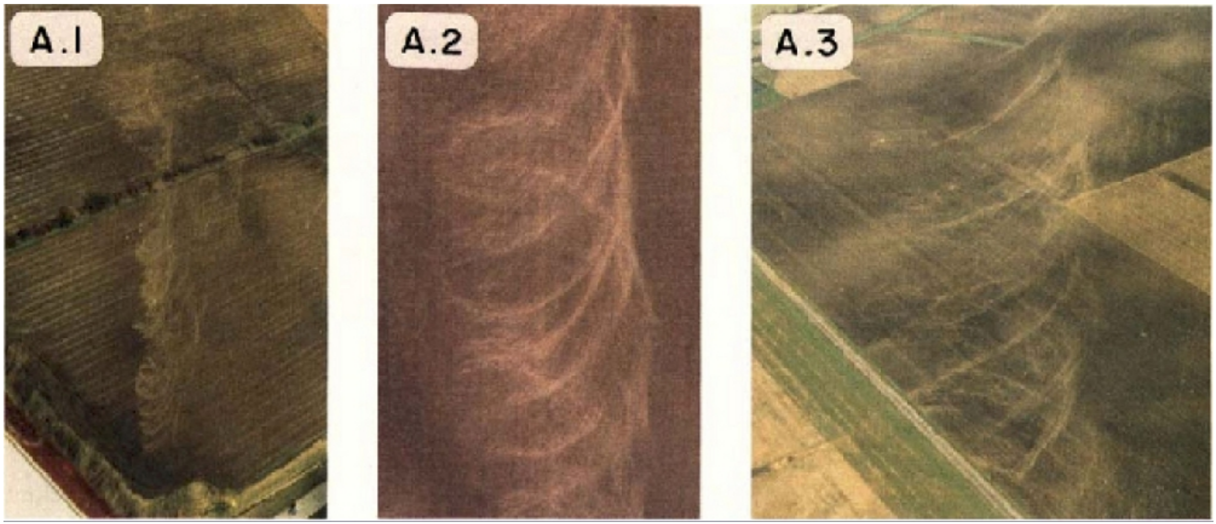

Figure 1: Aerial photography of surface marks from Fujita (1981).

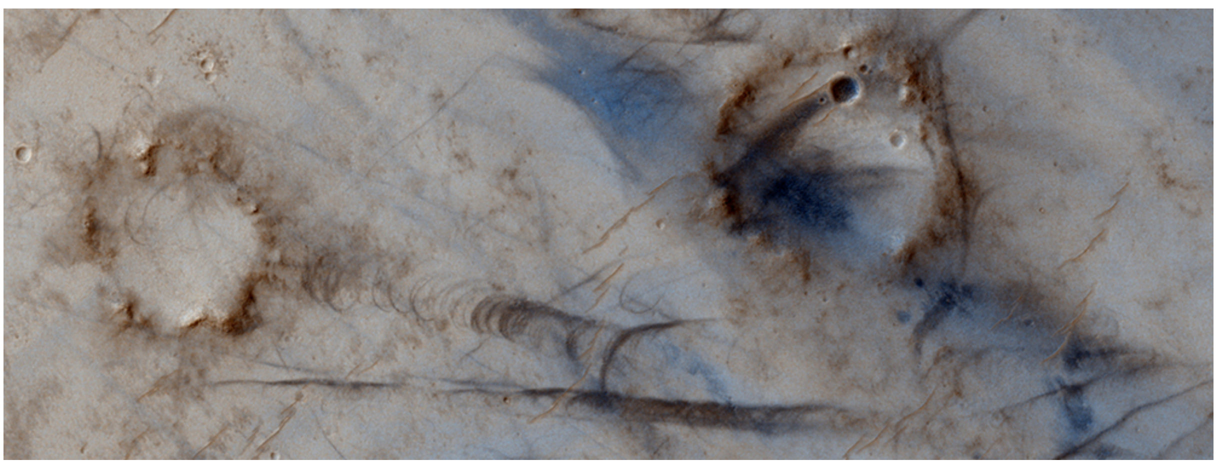

Figure 2: Martian dust devil tracks (horizontal dimension is about 500 m) [Image: NASA/JPL/University of Arizona].

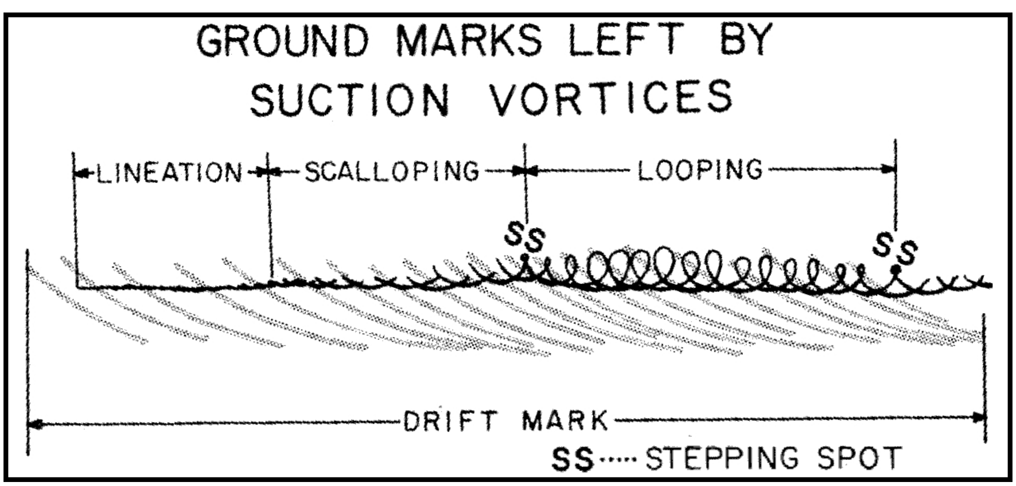

Figure 3: The surface mark taxonomy of Fujita et al. (1976).

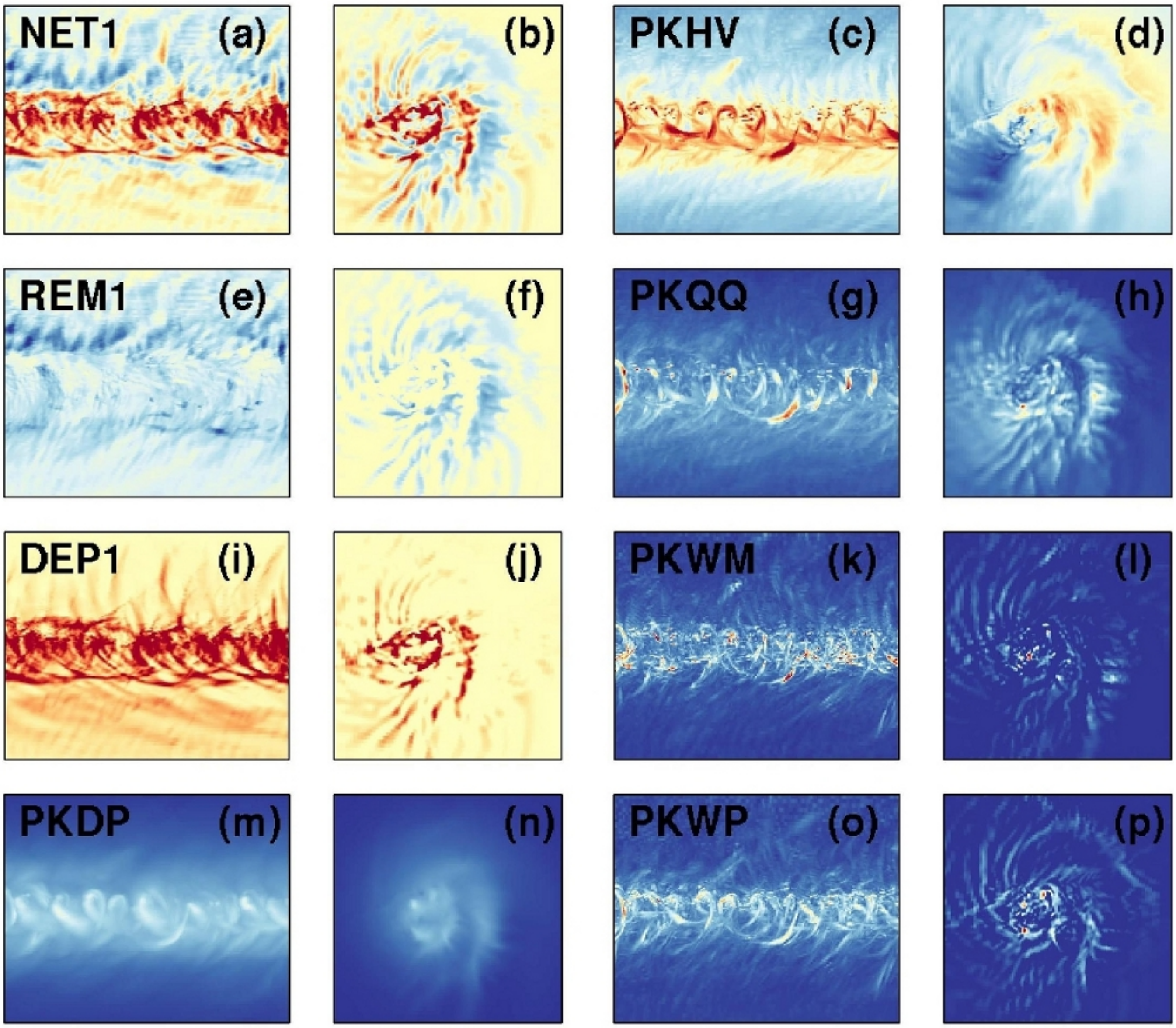

Figure 4: Surface tracks with sample instantaneous flow fields for a high-swirl tornado moving to the right at 25 m/s. (a,b) Net deposition track and instantaneous surface debris flux (red/blue=deposition/removal), (e,f) total removal and instantaneous upward surface debris flux, (i,j) total deposition and instantaneous downward surface debris flux. Also shown are peak measures and plots of instantaneous (c,d) horizontal air velocity at $z = 0.5$ m height, (g,h) subgrid turbulent kinetic energy at $z = 0.5$ m, (k,l) downward vertical air velocity at $z = 0.5$ m, (m,n) hydrodynamic pressure drop at $z = 0.5$ m, (o,p) upward vertical air velocity at $z = 0.5$ m.

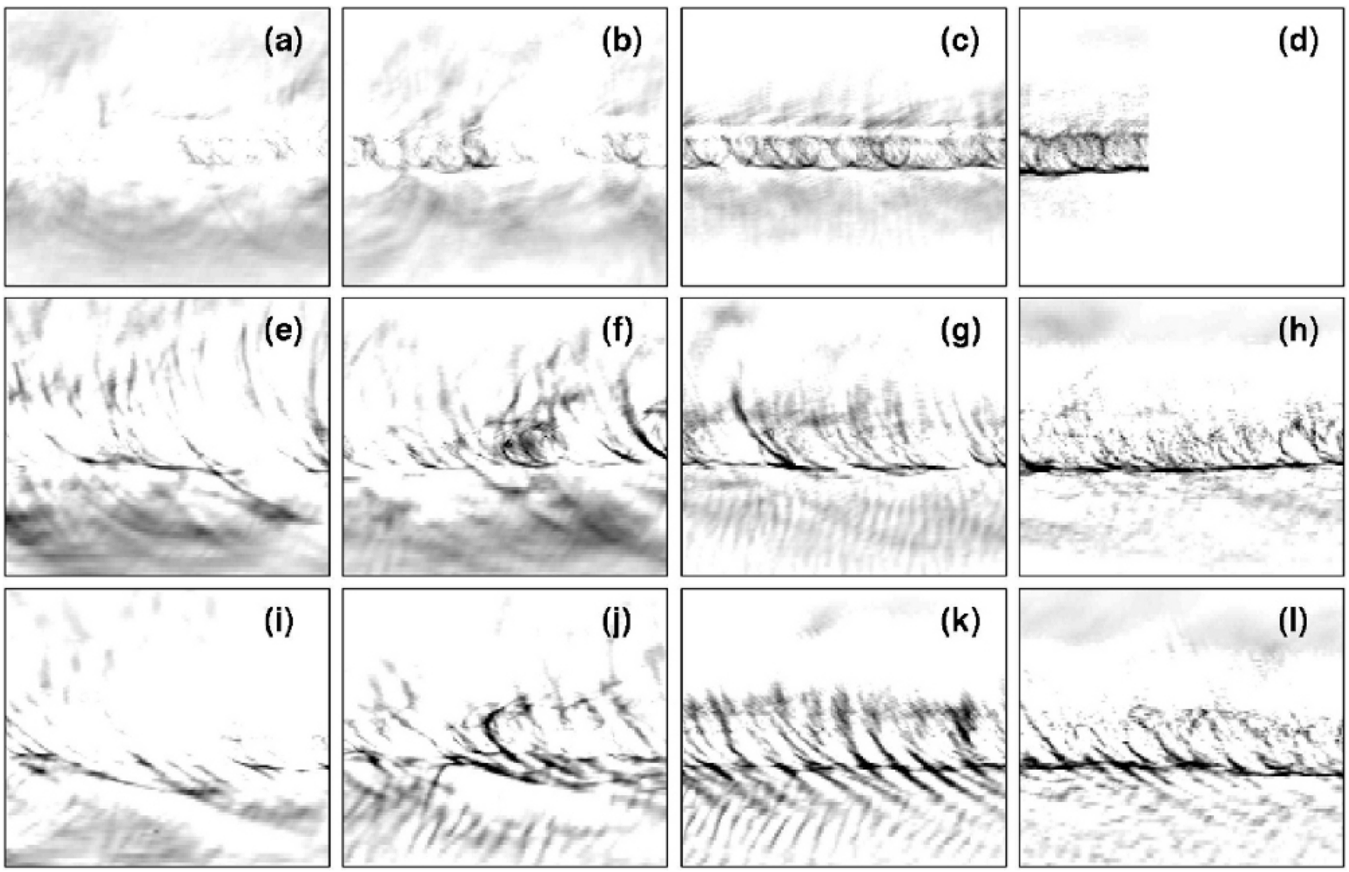

Figure 5: Deposition tracks from a collection of simulated tornadoes varying A_v and A_t for fixed $A_a = 7.9$ and $S_c = 3.0$. Left to right: $A_v = 24, 16, 11, 7.2$. Top to bottom: $A_t = 0.06, 0.17, 0.28$. Deposition intensities scaled by A_t. Spatial scale normalized to R_c aloft.

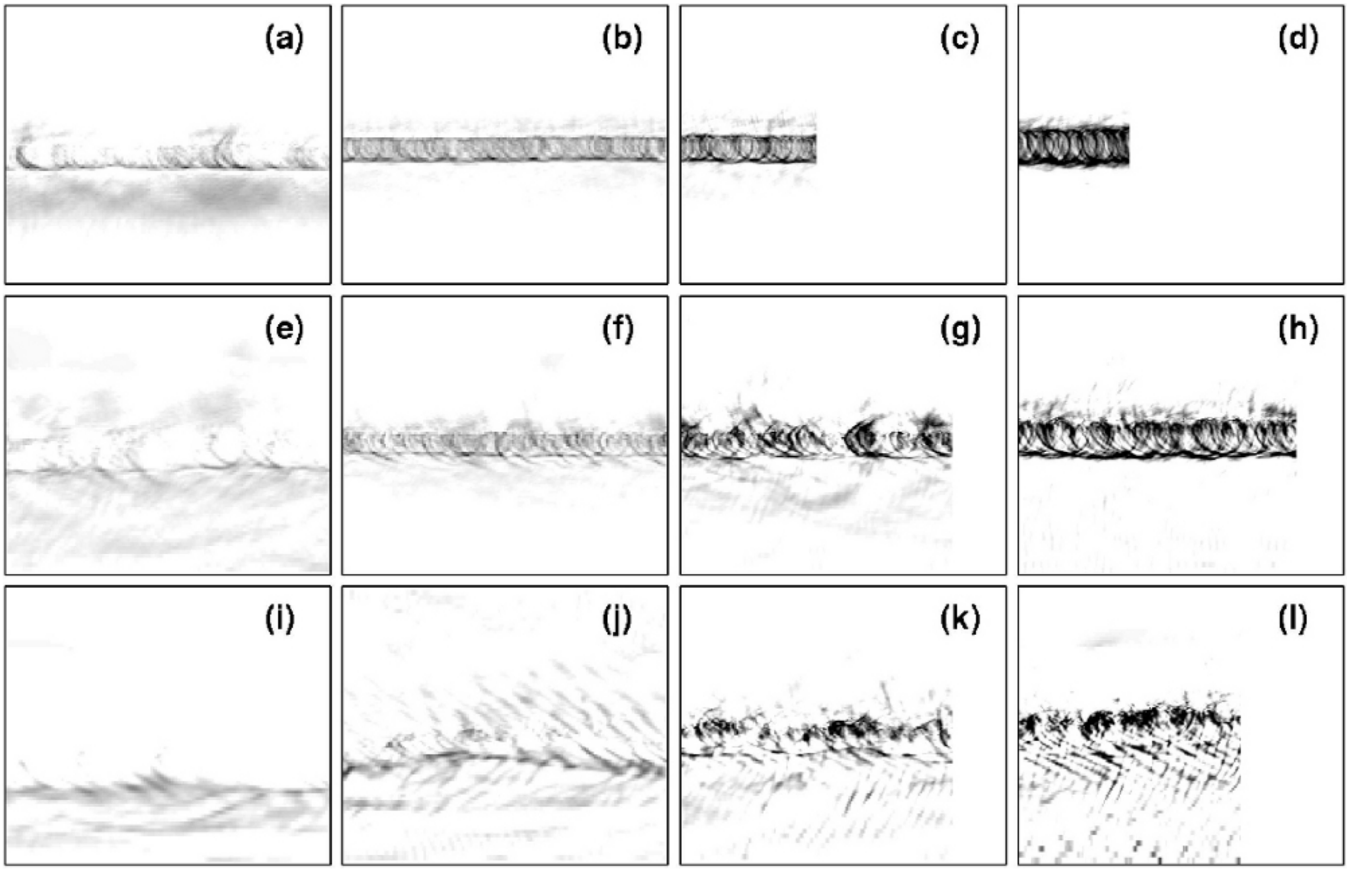

Figure 6: Deposition tracks from a collection of simulated tornadoes varying S_c and A_t for fixed $A_a \sim 2$ and $A_v \sim 8$. Left to right: $S_c = 1.9, 3.3, 5.6, 12.4$. Top to bottom: $A_t \sim 0.1, \sim 0.25, \sim 0.5$. Intensities scaled by A_t. Spatial scale normalized to R_c aloft.

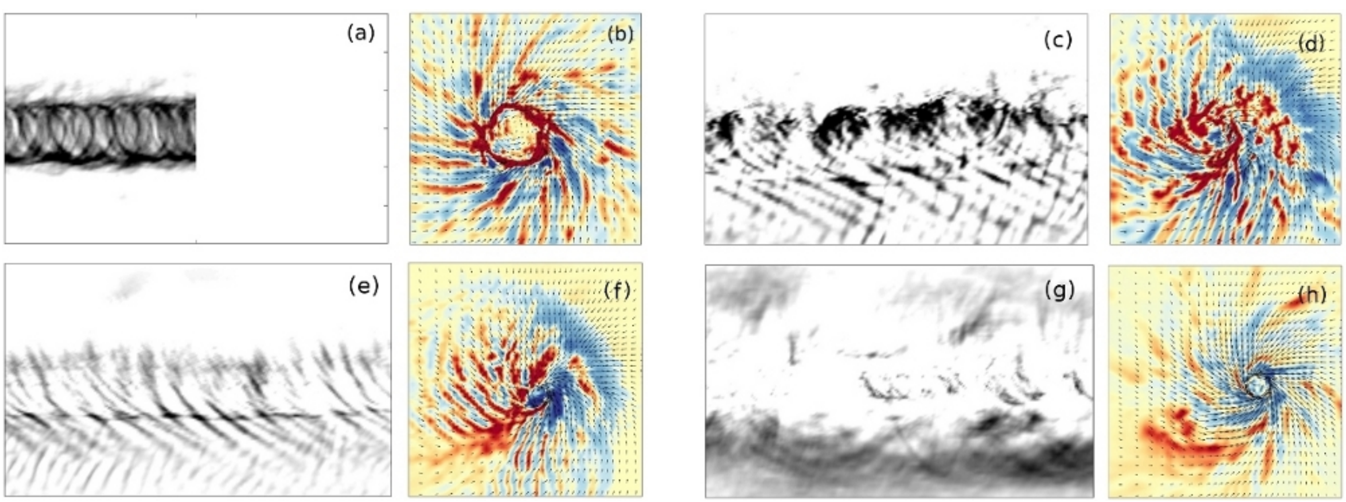

Figure 7: Deposition tracks with sample instantaneous vertical debris flux fields. Lateral dimensions are 600 m, dimensions along the direction of tornado translation are 1000 m. (a,b) $S_c = 12.4$, $A_t = 0.072$, $A_v = 8.2$, $A_a = 2.4$; (c,d) same as (a,b) except $A_t = 0.50$; (e,f) $S_c = 3.0$, $A_t = 0.28$, $A_v = 11$, $A_a = 7.9$; (g,h) same as (e,f) except $A_t = 0.055$, $A_v = 23.8$. Cycloids are apparent in (a,c), trailing arcs (strong, slanted lines) and lineation (dash-like horizontal lines) in (c,e), diffuse far-field swaths in (g).

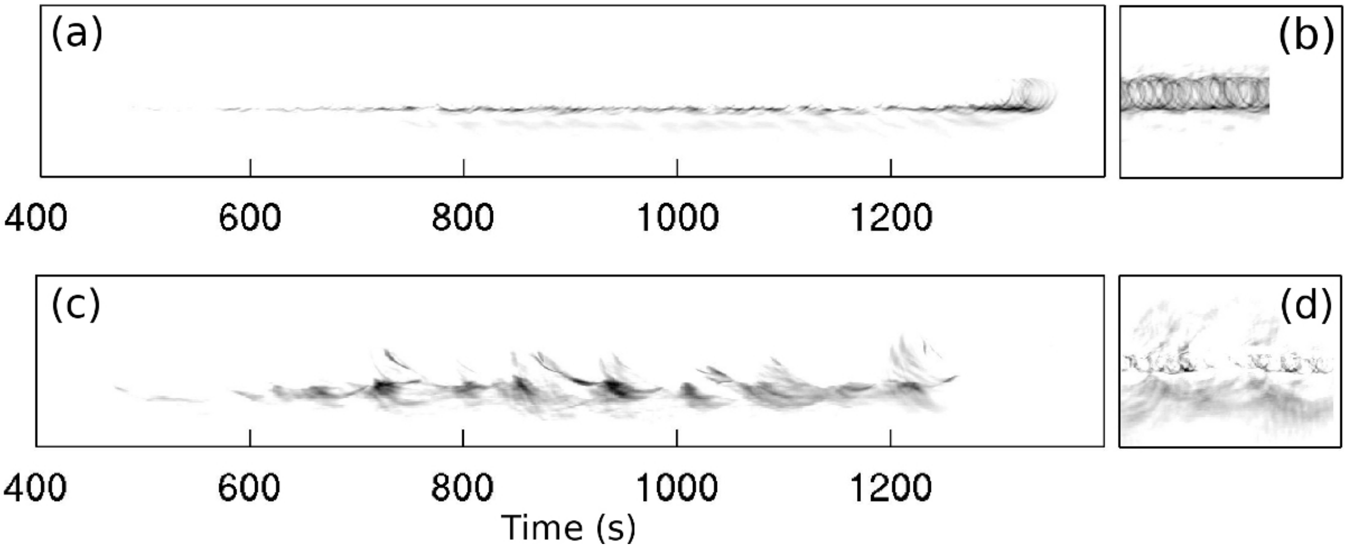

Figure 8: Deposition tracks for simulated tornadoes moving rightward at 5 m/s over a limited (1 kg/m^2) surface debris source (left column) and an unlimited surface debris source (right column). (a,b) High-swirl cases ($S_c = 12.4$, $A_t = 0.072$, $A_v = 8.2$, $A_a = 2.4$). (c,d) medium-swirl cases ($S_c = 3.0$, $A_t = 0.055$, $A_v = 15.9$, $A_a = 7.9$).

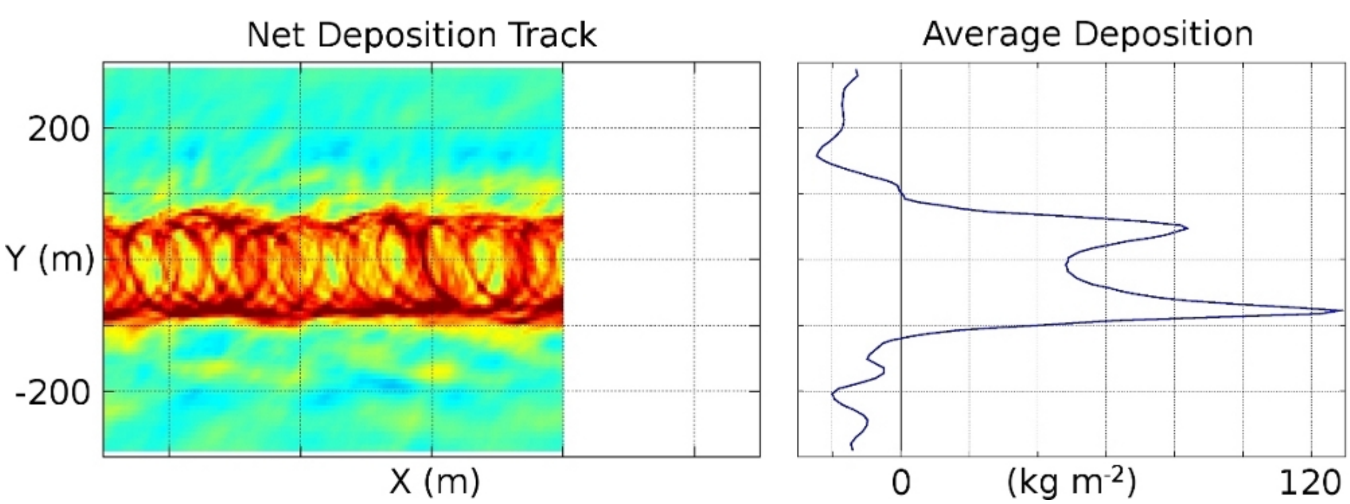

Figure 9: (a) Net deposition track for a high-swirl tornado moving at 5 m s^{-1} with (b) the downstream average of the net deposition pattern from (a), showing double-peaked structure that provides an estimate of the near-surface vortex radius.

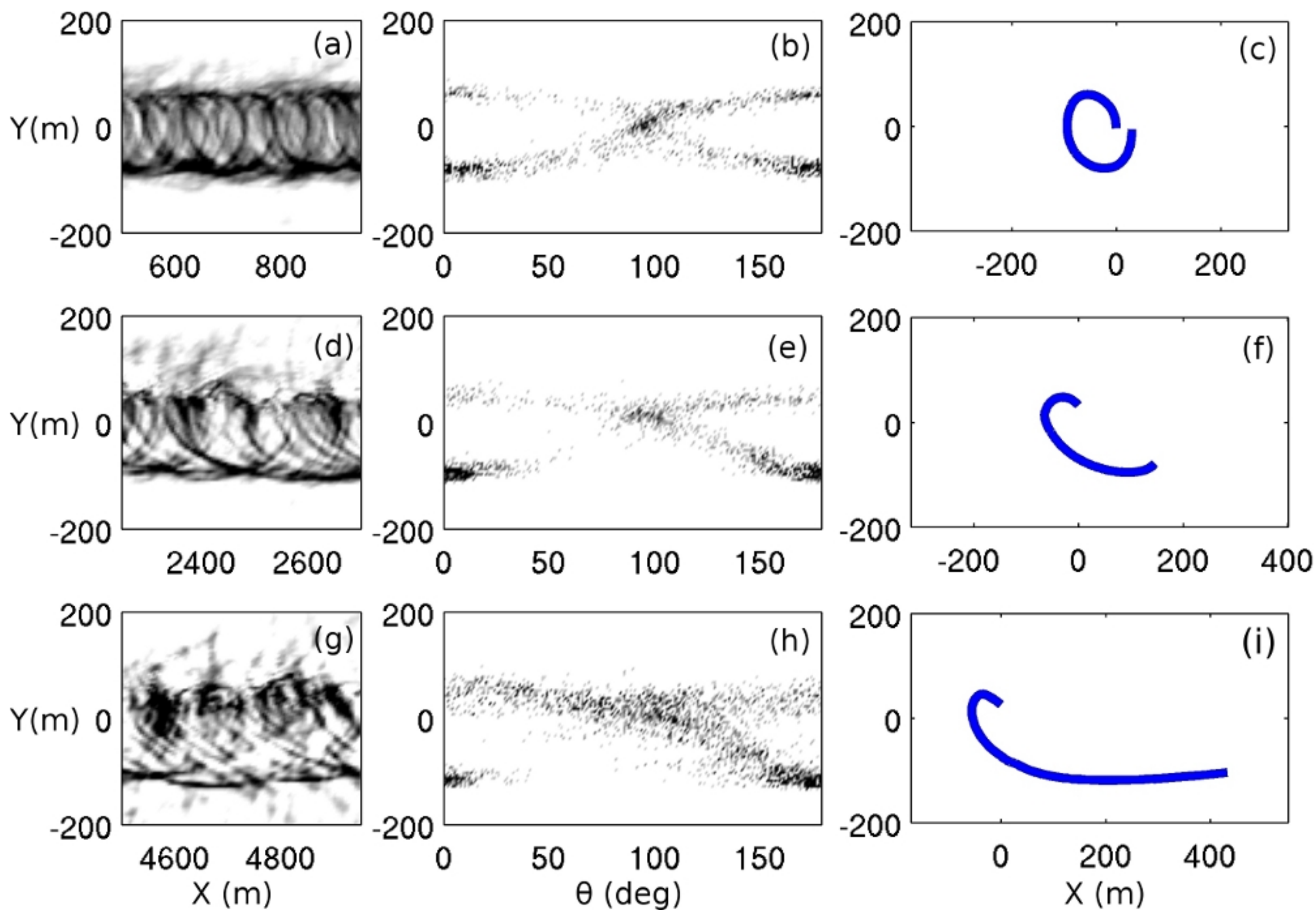

Figure 10: Shape analysis of deposition marks from simulated high-swirl tornadoes moving at (top row) 5 m/s, (middle row) 15 m/s, and (bottom row) 25 m/s. Left column: deposition tracks with intensities scaled by A_t. Middle column: orientation histograms. Right column: average “fingerprints” of the most prominent marks.